Effectiveness of stratospheric solar-radiation management as a function of climate sensitivity

Effectiveness of stratospheric solar radiation management as a function of climate sensitivity

Katharine L. Ricke*[1], Daniel J. Rowlands[2], William J. Ingrams[2,3], David W. Keith[4], and M. Granger Morgan[5]

1. Department of Global Ecology, Carnegie Institution for Science, 260 Panama Avenue, Stanford, CA 94305, USA.
2. Atmospheric, Oceanic and Planetary Physics, University of Oxford, Clarendon Laboratory, Parks Road, Oxford, OX1 3PU, UK.
3. Also at Met Office Hadley Centre, FitzRoy Road, Exeter, EX1 3PB, UK.
4. John F. Kennedy School of Government, Harvard University, 79 JFK Street, Cambridge, MA 02138, USA.
5. Department of Engineering & Public Policy, Carnegie Mellon University, 5000 Forbes Avenue, 129 Baker Hall, Pittsburgh, PA 15213, USA.

*kricke@stanford.edu

If implementation of proposals to engineer the climate through solar radiation management (SRM) ever occurs, it is likely to be contingent upon climate sensitivity. However, modeling studies examining the effectiveness of solar radiation management (SRM) as a strategy to offset anthropogenic climate change have used only the standard parameterizations of Atmosphere-Ocean General Circulation Models (AOGCMs) that yield climate sensitivities close to the Coupled Model Intercomparison Project (CMIP) mean. Here, we use a perturbed physics ensemble modeling experiment to examine how the response of the climate to SRM implemented in the stratosphere (SRM-S) varies under different greenhouse gas (GHG) climate sensitivities. When SRM-S is used to compensate for rising atmospheric concentrations of GHGs, its effectiveness in stabilizing regional climates diminishes with increasing climate sensitivity. However, the potential of SRM-S to slow down unmitigated climate change, even regionally, increases with climate sensitivity. On average, in variants of the model with higher sensitivity, SRM-S reduces regional rates of temperature change by more than 90 percent and rates of precipitation change by more than 50 percent.

The Royal Society has defined solar radiation management (SRM) as techniques that "attempt to offset effects of increased greenhouse gas concentrations by causing the Earth to absorb less solar radiation" [1]. The most plausible large-scale method is to increase the loading of light-scattering aerosols in the stratosphere (SRM-S) [1]. A number of AOGCM modeling studies suggest that SRM can compensate for many of the temperature and precipitation changes associated with global warming, even at the regional level [2-4], though these regional compensatory effects are not uniform [4,5]. These previous studies have used models in which the climate's equilibrium sensitivity to greenhouse gas forcing (henceforth, CS) reflects near-median estimates of CS. However, both observationally-constrained and expert-elicited estimates of CS have a substantial "high tail" [6,7] and it is arguably more likely that if SRM is deployed it will be because CS, and the impacts from climate change, turn out to be higher than current best estimates. Here we examine the effectiveness and side effects of SRM-S across a range of CS to check if use of the mean CS biases our understanding of SRM.

Evaluating the effectiveness of SRM-S requires first specifying the conditions in which it might be implemented and the effects that would be desired. There are various scenarios under which SRM might be employed. From a conventional policy viewpoint in which SRM is one of a portfolio of strategies alongside mitigation and adaptation, it could be used to minimize net social costs of climate change [8,9]. Alternatively, SRM is often framed as disaster insurance to be employed in case of the "extreme warming" that would occur under high CS [10] (and which may bring about "catastrophic" changes such as rapid deterioration of the Greenland ice sheet or large releases of methane from thawing permafrost [11]).

To investigate how SRM-S might be used to counterbalance future GHG-induced climate change in model variants with high CS that are also consistent with recent observed climate change, we perform a "perturbed physics" ensemble (PPE) modeling experiment with the HadCM3L AOGCM [12-15]. Like other PPEs [16,17], we simulate past and future climate scenarios using a wide range of model parameter combinations that both reproduce past climate within a specified level of accuracy but simulate future climates with a wide range of climate sensitivities. We chose 43 members ("model variants") from a subset of the 1,550 from the British Broadcasting Corporation (BBC) climate*prediction*.net (cpdn) project that have data that allow restarts (see Methods, Supplementary Methods and Supplementary Figure S1). [12,13]

Anthropogenic emissions were modeled using a mid-range standard emissions scenario, SRES A1B [18]. SRM-S is simulated in the model by specifying a globally uniform aerosol optical depth (AOD). The simulations run through 2000-2080 with SRM-S forcings applied from 2005. A first cpdn experiment using HadCM3L's standard physical parameters (i.e., the "standard physics" model variant) to look at global and regional responses to 135 different potential SRM-S scenarios [3] showed that, even regionally, changes to stratospheric AOD produce approximately colinear temperature and precipitation responses. Using the SRM-S scenarios that best stabilized global temperature in that experiment, we analyze the effects of four SRM-S scenarios (no-, low-, medium-, and high-SRM) to simulate with the PPE. The low-, medium- and high-SRM scenarios are designed to approximately counteract rising radiative forcing from anthropogenic emissions and stabilize global mean temperature within 1˚C relative to present day in all model variants (see Methods, Supplemental Methods and Figure S2). The no-SRM scenario used a constant stratospheric AOD corresponding to mean natural volcanic activity in the recent past. [19]

Figure 1 shows five-year-running-mean global-mean surface air temperature and precipitation rates for each model variant for the no-SRM, low-SRM and high-SRM scenarios. SRM cannot simultaneously compensate for the impacts of rising greenhouse gases on both temperatures and the hydrological cycle. Most of the effect of either SRM or GHGs on mean precipitation is via temperature, but if their effects on temperature are made to cancel, changes in mean precipitation are driven by the direct effects of their radiative forcings, both of which reduce precipitation (by reducing surface radiative heating and reducing tropospheric radiative cooling, respectively) [20, 21]. Under the no-SRM scenario, global-mean temperature and precipitation increased with all model variants. While results vary, both high- and low-SRM yield relatively stable temperatures after 2020 and show decreasing precipitation.

To analyze the regional impacts of different levels of SRM-S we examined mean temperature and precipitation anomalies over land in 23 "Giorgi regions" [22] (responses over the ocean are not displayed but tend to be similar). Results are presented for each PPE model variant using the projected warming without SRM-S from 2000 to 2050 as the independent variable. The projected warming is correlated with CS and the results of analyses presented in the following sections are the same if CS is used as the independent variable.

As an example of how regional responses to greenhouse gas and SRM-S forcings vary among model variants, Figure 2 shows decadal-mean temperature and precipitation changes between 2000 and 2050, normalized by the ensemble-mean inter-annual variability of control climates unperturbed by greenhouse gases or SRM, for just two regions and two model variants: the standard physics variant (ΔT_{2050}=2.1 C) and the ensemble's highest-warming variant (ΔT_{2050}=4.1 C).

With both model variants, Region 1 gets warmer and wetter under A1B, while Region 2 gets warmer and drier. When SRM-S is used, both regions move back towards their baseline climate states in both model variants. In the standard physics model variant, with the right amount of SRM-S, each region could return almost exactly to its 2000 baseline for both annual-average temperature and precipitation although the amount of forcing required is different for the two regions. In the high CS model variant, the closest each region can return to its baseline climate state is approximately one standard deviation. (These data points were selected for illustrative purposes, but are reasonably representative. Not all low sensitivity model variants return Region 1 and Region 2 so close to the origin, and some regions cannot be simultaneously returned to their baseline values of temperature and precipitation even in the standard physics model variant. See Supplementary Figures S3 and S4.)

The ensemble design allows analysis of the relationship between various regional measures of SRM-S efficacy and the overall global warming or CS of the model variant. Regional SRM-S efficacy-defined here as the fractional extent that SRM-S can return regional climates from the no-SRM case toward the baseline-can be expressed in both relative and absolute terms. These measures are averaged for presentation using three different weightings: each region is unweighted; each is weighted by its population; or each is weighted by its economic output. [23]

To assess the diversity of likely regional preferences for the amount of SRM-S, we first consider OD*, the change in optical depth that returns the region's climate closest to its baseline (the origin in Figure 2) in terms of combined interannual standard deviations of temperature and precipitation. We also consider regional anomalies (the variability-normalized regional temperature, precipitation, and combined temperature and precipitation changes) for variously weighted mean-OD* and the ratio of regional anomalies at global-mean-OD* to those associated with no SRM.

Analyzing precipitation rather than, for example, soil moisture to evaluate the effect of SRM-S on the hydrological cycle does not seem to result in a systematic overestimation of its efficacy. For example, as the amount of SRM-S increases, regional precipitation anomalies associated with anthropogenic emissions, are generally ‘overcorrected’ (SRM changing the sign of the anomaly compared with the no-SRM case) before runoff (precipitation minus evaporation) anomalies are.

Precipitation and temperature changes, albeit very important, are only two of the many variables likely to have climate related impacts. The potential for moderating effects such as sea level rise and ice sheet melt (while more difficult to accurately model in AOGCMs) will also be relevant to decisions by some parties about whether to implement SRM-S. As such, our SRM efficacy metrics are useful indicators of tradeoffs that occur when attempting to stabilize regional GHG-driven climate changes using SRM-S, but are not definitive normative measures of regional impacts or likely preferences. Because our simulations do not include 'threshold' effects such as collapse of the thermohaline overturning or catastrophic release of methane, our metrics also cannot measure the ability of SRM-S to counteract the type of forcing feedbacks that would occur if certain climate tipping points were surpassed [24] before SRM-S implementation.

Ten-year mean values of various efficacy measures against model variant temperature response for decades averaged around 2030, 2050 and 2070 are shown in Figure 3 and in Supplementary Figures S5 and S6. As greenhouse gas concentrations rise, more SRM-S is required to compensate (Figure 3). Mean regional preferences for the amount of optical depth modification (i.e., mean-OD*) are fairly insensitive to modelled

CS regardless of weighting. This should be expected physically because a model variant more sensitive to one radiative forcing is generally similarly sensitive to the other radiative forcing and SRM-S is used to cancel roughly the same amount of forcing regardless of the modelled CS. Results are similar using median-OD* rather than mean. Trends for seasonal data are similar, though the economic output weighted slopes do change noticeably because economic output is concentrated in the Northern Hemisphere (not shown).

The standard deviation of regional preferences for OD* (Supplementary Figure S7) decreases with modelled temperature response. This should also be expected physically as the smaller variation in the strength of SRM-S would have more impact if climate sensitivity were higher.

However, the mean and standard deviation of regional anomalies at mean-OD* increase with modelled warming (Supp Figure S5), again regardless of weighting. On average across the ensemble, at OD* these SRM-modified climates are slightly warmer and drier than their baseline climates, as is physically expected [21,22]. The higher regional anomalies are driven by amplified regional drying in high-CS worlds; there is no statistically significant relationship between modelled warming and the magnitude of regional *temperature* anomalies with SRM-S set at mean-OD*. As a proxy for regional impacts with SRM, the higher mean anomalies imply that SRM-S is less effective overall as a substitute for mitigation in higher sensitivity worlds – precisely when SRM-S seems most likely to be deployed. Higher standard deviations of regional anomalies in higher CS model variants also suggest interregional heterogeneities associated with an SRM-S substitution would be greater in higher sensitivity worlds.

Conversely, the mean and the standard deviation of the ratio of regional anomalies at mean-OD* to anomalies with no SRM-S decrease with modelled CS and decrease over the length of the simulations (Supp Figure S6). By these measures, SRM-S is more effective and equitable at reducing the risk from climate change when CS is high.

From some impacts perspectives, rates of regional climate change matter more than absolute anomalies [25,26]. On average, without SRM-S, regional rates of warming and precipitation change are more than twice as high in the ensemble's highest sensitivity model variants as in the lowest sensitivity model variants and are similar in magnitude to the regional rates of change simulated by the same variant between 1996-2005. With SRM-S applied, the rates of temperature change are insensitive to the modelled CS (Figure 4a). Rates of precipitation change are marginally (but statistically significantly) higher in higher CS model variants (Figure 4c), but on average, SRM-S reduces regional rates of temperature change by more than 90% and rates of precipitation change by more than 50% in the highest CS model variants (forecast warming greater than 3.5°C). The ability of SRM-S to reduce rates of change in the face of high CS does not depend strongly on the inter-regional weighting scheme, implying that while divisions between Giorgi regions are socioeconomically meaningless, the average responses of the regions are still meaningful. Effectiveness also does not depend on the decade, implying that the effectiveness of SRM-S in reducing change is roughly independent of when it is implemented.

Given the regional heterogeneity of SRM-S effectiveness and the fact that it will only moderate, never eliminate regional climate changes, it is unlikely that all regions would find their local outcomes comparably satisfactory, and many regions may find the result increasingly unsatisfactory over time. Conceivably some regions will prefer their new climates to those of 2000. In addition there are other risks (such as potential for stratospheric ozone depletion [27, 28]) and imperfections (such as a failure to address ocean acidification [29]) associated with SRM-S which may also vary with CS.

We have explored how much existing assessments of SRM-S, by using standard GCMs with near-median CS, may ignore important contingencies. As noted above, a major motivation for studying SRM is to evaluate its potential effectiveness as insurance against higher-than-expected sensitivity of climate to radiative forcing due to greenhouse gases. We find that SRM-S is least effective in returning regional climates to their baseline states and minimizing regional rates of precipitation change under precisely such high CS conditions. On the other hand, given the very high regional temperature anomalies associated with rising greenhouse gas concentrations under high CS, this is also where SRM-S is most powerful in reducing change relative to the no SRM-S alternative.

METHODS

Ensemble Design

The standard versions of AOGCMs have generally benefited from considerable tuning: the set of values of model parameters has been developed to give physically-based realistic simulations. A PPE deliberately "detunes" the model, setting parameters to any physically plausible value, to explore uncertainty space. Many of the original 1,550 climate*prediction*.net model variants thus provide a poor simulation of recent observed climate change. We aim to use only model variants that provide a credible simulation of the past 50 years while maintaining a large diversity in the response in 2050. A number of the choices we made in the design are for pragmatic reasons rather than being based on a formal sampling algorithm, since we do not seek to interpret the distribution of model variants in the new ensemble in any probabilistic terms. Several factors were considered in selecting model variant runs.

First, we held constant the future solar forcing scenario [30], and the future anthropogenic sulphate emissions trajectory. To avoid discontinuities in the solar forcing at the year 2000 we only consider simulations with a solar forcing very close to the chosen scenario in 2000. Second, we only used model variants with a relatively stable base climate. We eliminated model variants in which the initial-condition ensemble average of the control simulations exhibited a drift greater than 0.5K/century fitted over 1960-2080. Finally, we selected model variants through a comparison of the modelled and observed spatio-temporal pattern of temperature change over the past 50 years (see Supplementary Methods).

Supplementary Figure S1 plots the goodness of fit between models and observations against simulated warming in 2050 with our forty-three-member PPE ensemble. The colour code for those points indicates the model's calculated equilibrium climate sensitivity from corresponding equilibrium slab ocean simulations, which is correlated with transient warming (see Supplementary Methods).

To select a subset of the models for inclusion in the new ensemble that ensured a wide range of responses in the future, models were binned by projected warming in 2050 into 10 equally spaced bins spanning the range of responses. In each bin, the model variant with the lowest r^2 was automatically included, along with 4 others sampled probabilistically (see Supplementary Methods), avoiding duplicates. In the two highest response bins there were less than 5 model variants that met the selection criteria, and hence our selection yielded only 43 model variants.

A 10-member initial condition ensemble was generated for each model variant. (see Supplementary Methods) For our analysis, the 430-member ensemble was run for each of the 4 SRM-S scenarios, giving a total of 1720 model simulations.

SRM Forcings

SRM-S activities were simulated by specifying globally uniform variations in stratospheric optical depth. This is distributed in the vertical proportional to the mass of air in each stratospheric level in each level above the tropopause, which is diagnosed for each point and timestep using a lapse-rate-based criterion [31].

A baseline SRM-S scenario (medium-SRM) was formulated using the results from the standard physics experiment [3] in which 135 SRM-S scenarios were formulated, designed to offset the net forcings associated with long-lived greenhouse gases, tropospheric sulphur aerosols and tropospheric ozone; and spanning the uncertainties associated with these anthropogenic forcings. The two scenarios which best stabilized global surface air temperature in that experiment according to a least-squares fit analysis were averaged. In the no-SRM scenario, stratospheric AOD was set to 0.01 (at 0.55 microns, the reference wavelength [31]), a level approximately equal to mean volcanic activity in the recent past [19], over the entire length of the simulations. The high-SRM-S and low-SRM-S scenarios are the same as the baseline SRM-S scenario except for the addition (0.075) or subtraction (0.015) of a constant amount of optical depth at all points in the simulations (see Supplementary Figure S2 and Supplementary Methods).

Statistical Analysis

For each of the 43 model variants we average output over a 10-member initial condition ensemble to improve the signal-to-noise ratio. All best fits shown were fitted using least-squares regression. (See Supplementary Table S1 for all regression coefficients and corresponding p-values.) The latter are calculated using standard assumptions including Gaussian noise, which may be misleading, particularly in the far tails. We therefore do not specify p-values beyond 2 decimal places.

Regional Population and Economic Weightings

Population and economic output data for the year 2005 were obtained from the Nordhaus G-Econ dataset, which contains gross output and population at a 1°x 1° resolution and mapped onto the 22 "Giorgi regions," plus New Zealand [23].

Acknowledgments The authors thank the climate*prediction*.net participants for their donations of computing power without which the experiment would not have been possible. We thank M.R. Allen for advice in the design of the experiment, M.I. Thurston and N.R. Massey for deployment of the experiment through the cpdn system and J.B. Moreno-Cruz and two anonymous referees for thorough & valuable comments on the manuscript. KLR acknowledges support from a US National Science Foundation Graduate Research Fellowship. DJR was supported by a NERC PhD studentship with a

CASE award from CEH Wallingford. WJR was supported by NERC contract NE/D012287/1 and EU FP6 contract 036946. KLR, DWK and MGM acknowledge the support of the Climate Decision Making Center (SES-0345798) and the Center for Climate and Energy Decision Making (SES-0949710), both funded by the US National Science Foundation.

Contributions KLR and DR designed the experiment. KLR performed the data analysis. KLR, DR, WJI, DWK and MGM discussed the results and wrote the paper.

Competing financial interests The authors declare no competing financial interests.

1. The Royal Society, *Geoengineering the Climate: Science, governance and uncertainty*, 82pp., September 2009. Available on line at: royalsociety.org/WorkArea/DownloadAsset.aspx?id=10768.
2. Caldeira, K. & Wood, L. Global and Arctic climate engineering: numerical model studies. *Philos Transact A Math Phys Eng Sci* **366**, 4039-4056 (2008).
3. Moreno-Cruz, J. B., Ricke, K. L. & Keith, D. W. A simple model to account for regional inequalities in the effectiveness of solar radiation management. *Climatic Change* Doi: 10.1007/s10584-011-0103-z (in the press)
4. Ricke, K. L., Morgan, M. G. &Allen, M. R. Regional climate response to solar radiation management *Nature Geoscience* **3,** 537-541 (2010).
5. Jones, A., Haywood, J., Boucher, O., Kravitz, B., & Robock, A. Geoengineering by stratospheric SO_2 injection: Results from the Met Office HadGEM2 climate model

and comparison with the Goddard Institute for Space Studies ModelE. *Atmos. Chem. Phys. Discuss.* **10**, 7421-7434, (2010).

6. Roe, G. H. & Baker, M. B. Why is climate sensitivity so unpredictable? *Science* **318**, 629-632 (2007).
7. Zickfeld, K, Morgan, M.G, Frame, D. J, & Keith, D. W. Expert judgments about transient climate response to alternative future trajectories of radiative forcing. *Proc. Natl. Acad. Sci.* **107,** 12451-12456 (2010).
8. Wigley, T.M.L. A combined mitigation/geoengineering approach to climate stabilization. *Science* **314**, 452-454 (2006).
9. Moreno-Cruz, J. B. & Keith, D. W. Climate policy under uncertainty a case for geoengineering. (submitted to *Climatic Change*)
10. Victor, D.G. *Global Warming Gridlock* Ch. 6 (Cambridge University Press, 2011)
11. Blackstock, J. J. et al., *Climate Engineering Responses to Climate Emergencies* (Novim, 2009), archived online at: http://arxiv.org/pdf/0907.5140M.
12. Frame, D. J. et al. The climate*prediction*.net BBC climate change experiment: design of the coupled model ensemble. *Proc. R. Soc. A* **367**, 855-870 (2009).
13. Rowlands, D. J. et. al. Predictions of 21st century warming constrained by recent climate observations. (submitted to *Nature Geoscience*)
14. Gordon, C. et al. The simulation of SST, sea ice extents and ocean heat transports in a version of the Hadley Centre coupled model without flux adjustments. *Climate Dynamics* **16**, 147-168 (2000).
15. Allen, M.R. Do-it-yourself climate prediction. *Nature* **401**, 642-642 (1999).
16. Murphy, J. M. et al. Quantification of modelling uncertainties in a large ensemble of

climate change simulations. *Nature*, **430** (7001) 768–772 (2004).

17. Stainforth, D. A. et al. Uncertainty in predictions of the climate response to rising levels of greenhouse gases. *Nature* **433** (7024) 403–406 (2005).

18. Nakicenovic, N. et al. *IPCC Special Report on Emissions Scenarios*. pp 570. (Cambridge University Press, 2000)

19. Sato, M., Hansen, J.E., McCormick, M.P. & Pollack, J.B. Stratospheric aerosol optical depth, 1850-1990. *J. Geophys. Res.* **98**, 22987-22994, (1993).

20. Allen, M.R. & Ingram, W.J. Constraints on future changes in climate and the hydrologic cycle. *Nature* **419**, 224-232 (2002).

21. Bala, G., Duffy, P.B. & Taylor, K.E. Impact of geoengineering schemes on the global hydrological cycle. *Proc. Natl. Acad. Sci. U.S.A* **105**, 7664-7669 (2008).

22. Giorgi, F. & Francisco, R. Uncertainties in regional climate change prediction: a regional analysis of ensemble simulations with the HADCM2 coupled AOGCM. *Climate Dynamics* **16**, 169-182 (2000).

23. Nordhaus, W. Geography and macroeconomics: new data and new findings. *Proc. Natl. Acad. Sci. U.S.A* **103**, 3510-3517 (2006).

24. Lenton, T.M. et al. Tipping elements in the Earth's climate system. *Proc. Natl. Acad. Sci. U.S.A* **105,** 1786–1793 (2008).

25. Leemans, R & Eickhout, B. Another reason for concern: regional and global impacts on ecosystems for different levels of climate change, *Global Environmental Change*, **14,** 219-228 (2004).

26. Visser, M.E. Keeping up with a warming world; assessing the rate of adaptation to climate change. *Proc. R. Soc. B* **275,** 649-659 (2008).

27. Tilmes, S., Garcia, R.R., Kinnison, D.E., Gettelman, A. & Rasch, P.J. Impact of geoengineered aerosols on the troposphere and stratosphere. *J. Geophys. Res.* **114,** D12305 (2009).

28. Kirk-Davidoff, D. B., Hintsa, E. J., Anderson, J. G. & Keith, D. W. The effect of climate change on ozone depletion through changes in stratospheric water vapour. *Nature* **402,** 399-401 (1999).

29. Hoegh-Guldberg, O. et al. Coral reefs under rapid climate change and ocean acidification. *Science* **318,** 1737–1742 (2007).

30. Solanki, S. K. & Krivova, N. A. Can solar variability explain global warming since 1970? *J. Geophys. Res*., **108,** 1200 (2003).

31. Cusack S., A. Slingo, J.M. Edwards, and M. Wild, 1998; The radiative impact of a simple aerosol climatology on the Hadley Centre GCM. *QJR Meteor. Soc.* **124,** 2517-2526.

Figure 1. Time series of temperature and precipitation of the no-SRM, low-SRM and high-SRM scenarios examined, with initial condition sub-ensembles averaged for each of the 43 PPE model configurations analyzed. (a) Five-year running-mean global mean near-surface (1.5 m) air temperature, and (b) five-year running-mean global mean precipitation rate, all displayed over the length of the 80 model-year simulations.

Figure 2. Example of regional responses to A1B and SRM-S forcings in units of standard deviations for two model variants and two regions. Region 1 is Eastern North America; Region 2 is Southern Europe/Northern Africa. Blue-edged points show the no-SRM (black-centre), low-SRM (green-centre) and high-SRM (magenta-centre) responses for the standard physics model variant (ΔT_{2050}=2.1 C). Orange-edged points corresponding responses for the ensemble's highest sensitivity model variant (ΔT_{2050}=4.1 C). Temperature and precipitation anomalies are the difference between ten-year averages centered on 2050 and 2000, divided by the interannual variability of the control climate. Arrows indicate the trajectory as SRM-S increases.

Figure 3. Mean regional values of OD*, the amount of optical depth modification that returns each regional climate closest to its baseline state (the origin in Figure 2), plotted against 2050 forecast warming of the model variant for decadal means about 2030, 2050 and 2070. Points show the mean-OD* for each model variant when equal weight has been given to each of the 23 regions. Solid lines show best fits to these points. Dashed and dotted lines show best fits to points (not shown) that result if each geographic region is weighted by its economic output (dotted) or by its population (dashed).

Figure 4. The mean value of the absolute values of regional rate of change (a and c) and standard deviation of regional rates of change (b and d) for temperature **(a-b)** and precipitation **(c-d),** shown for both the medium-SRM (see Methods) and no-SRM scenarios for decadal intervals centered on 2030 (red), 2050 (black) and 2070 (blue), plotted against model forecast warming. In the case of precipitation, points and best-fit lines for the No-SRM simulations are shaded more lightly to distinguish them from the medium-SRM simulations.

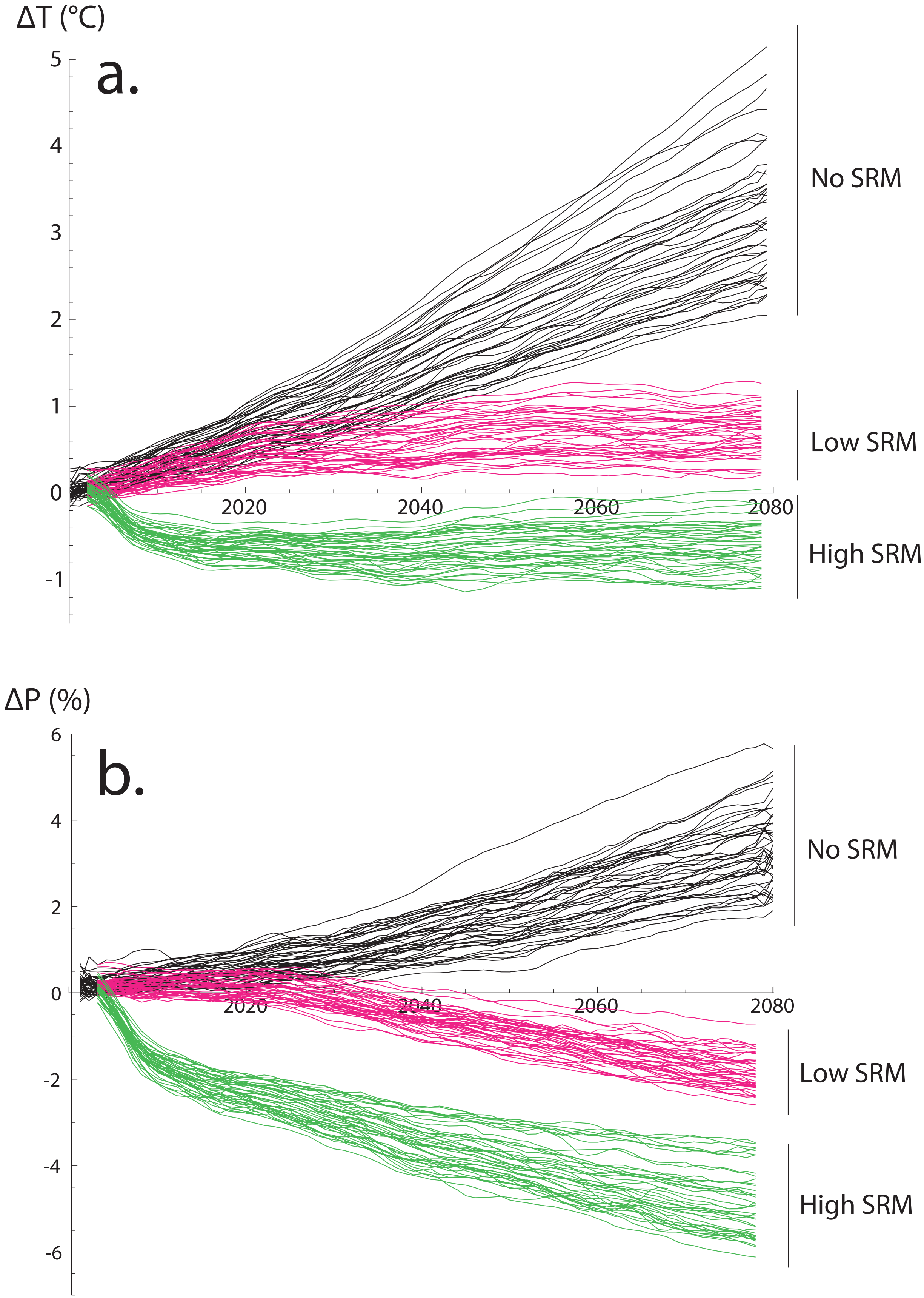

ΔT (°C)
a.
5
4
3
2
1
0
-1
2020
2040
2060
2080
No SRM
Low SRM
High SRM
ΔP (%)
b.
6
4
2
0
-2
-4
-6
2020
2040
2060
2080
No SRM
Low SRM
High SRM

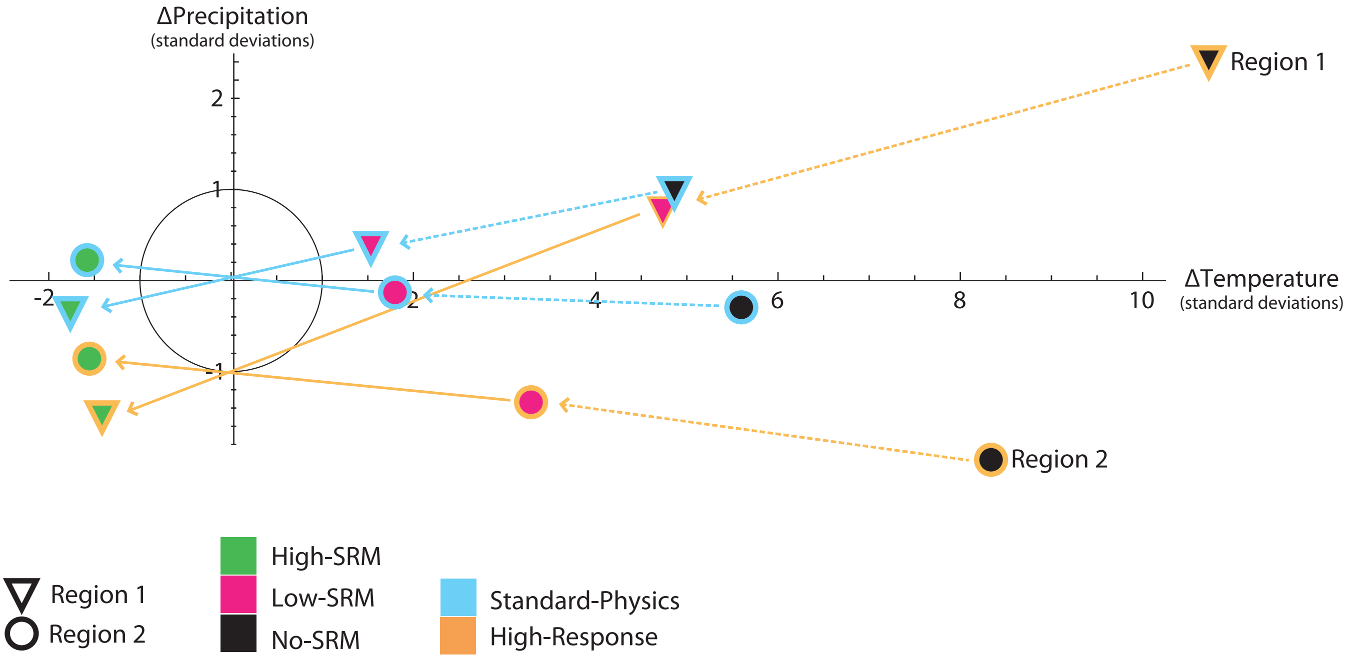

ΔPrecipitation
(standard deviations)
2
1
-1
-2
2
4
6
8
10
ΔTemperature
(standard deviations)
Region 1
Region 2
Region 1
Region 2
High-SRM
Low-SRM
No-SRM
Standard-Physics
High-Response

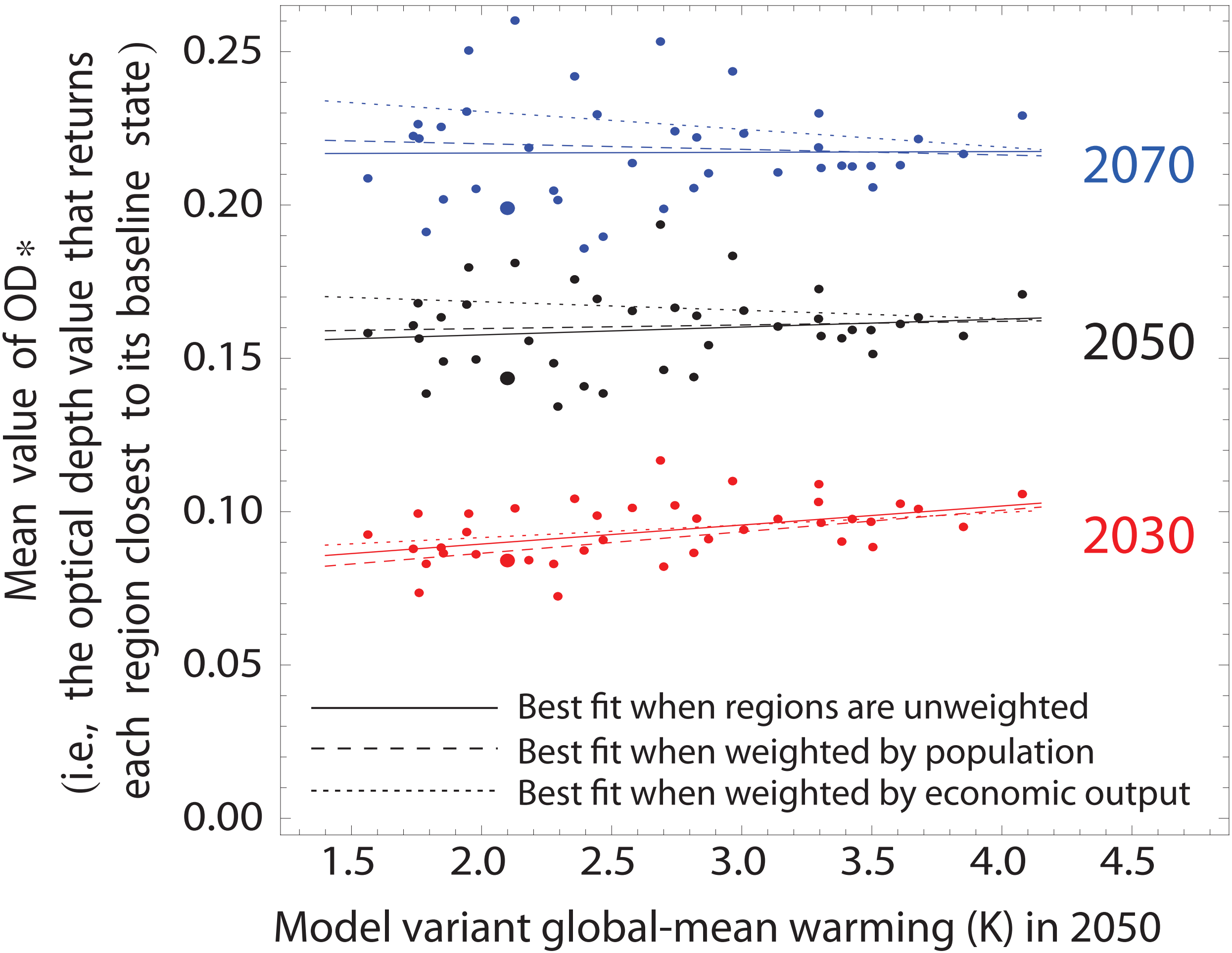
Mean value of OD*
(i.e., the optical depth value that returns
each region closest to its baseline state)
0.25
0.20
0.15
0.10
0.05
0.00
2070
2050
2030
Best fit when regions are unweighted
Best fit when weighted by population
Best fit when weighted by economic output
1.5
2.0
2.5
3.0
3.5
4.0
4.5
Model variant global-mean warming (K) in 2050

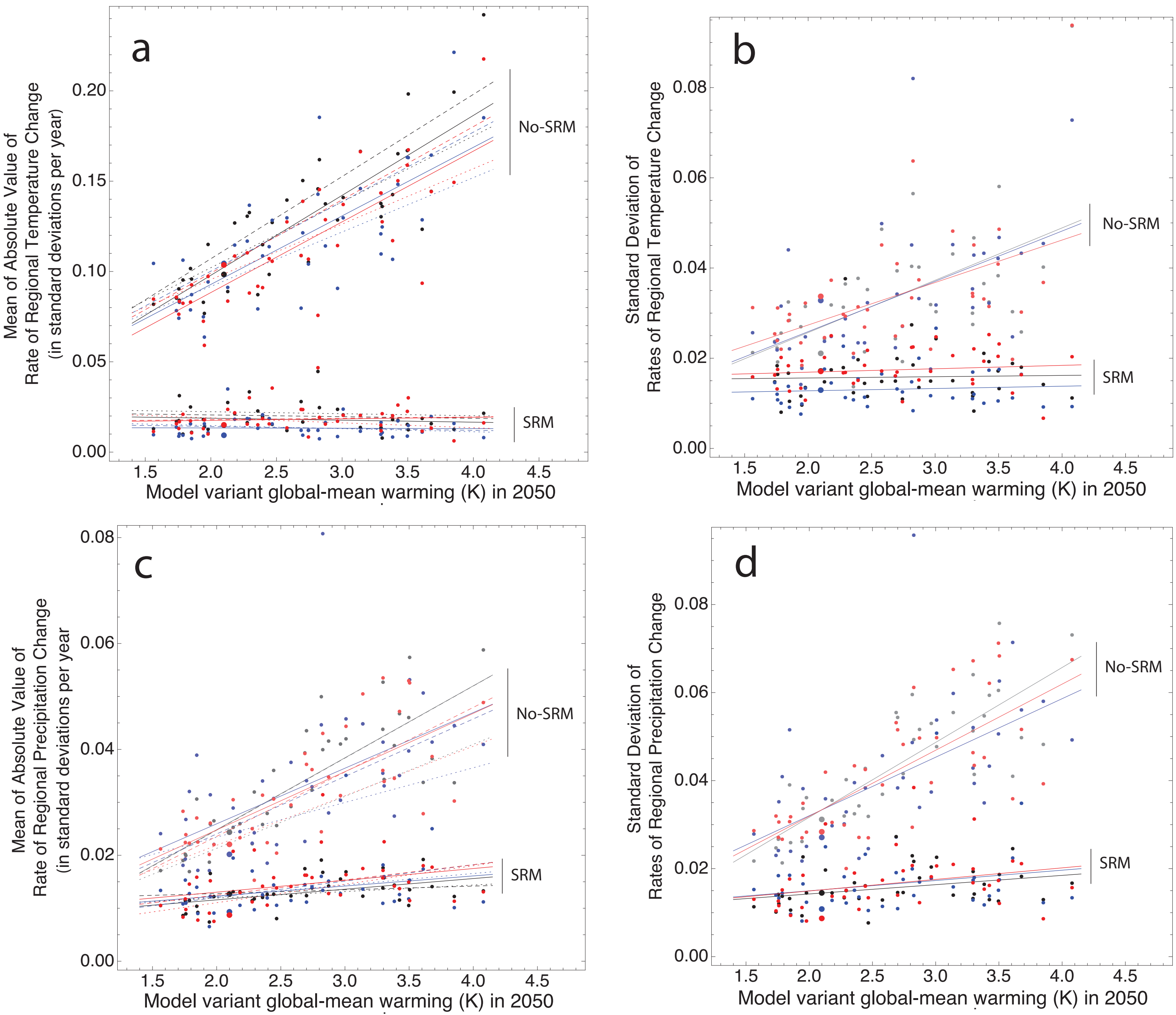
a
Mean of Absolute Value of
Rate of Regional Temperature Change
(in standard deviations per year)
0.00
0.05
0.10
0.15
0.20
No-SRM
SRM
1.5
2.0
2.5
3.0
3.5
4.0
4.5
Model variant global-mean warming (K) in 2050
b
Standard Deviation of
Rates of Regional Temperature Change
0.00
0.02
0.04
0.06
0.08
No-SRM
SRM
Model variant global-mean warming (K) in 2050
c
Mean of Absolute Value of
Rate of Regional Precipitation Change
(in standard deviations per year
0.00
0.02
0.04
0.06
0.08
No-SRM
SRM
Model variant global-mean warming (K) in 2050
d
Standard Deviation of
Rates of Regional Precipitation Change
0.00
0.02
0.04
0.06
0.08
No-SRM
SRM
Model variant global-mean warming (K) in 2050